Journal of Cellular Biochemistry 100:315–325 (2007)

TGFβ Inducible Early Gene-1 (*TIEG1*) and Cardiac Hypertrophy: Discovery and Characterization of a Novel Signaling Pathway

Nalini M. Rajamannan,[1]* Malayannan Subramaniam,[2] Theodore P. Abraham,[3] Vlad C. Vasile,[4] Michael J. Ackerman,[3,4,5] David G. Monroe,[2] Teng-Leong Chew,[6] and Thomas C. Spelsberg[2]

[1]Division of Cardiology, Northwestern University Feinberg School of Medicine, Chicago, Illinois
[2]Department of Molecular Biology and Biochemistry, Mayo Clinic College of Medicine, Chicago, Illinois
[3]Department of Medicine/Division of Cardiovascular Disease, Mayo Clinic College of Medicine, Chicago, Illinois
[4]Department of Molecular Pharmacology and Experimental Therapeutics, Mayo Clinic College of Medicine, Chicago, Illinois
[5]Department of Pediatrics/Division of Pediatric Cardiology, Mayo Clinic College of Medicine, Chicago, Illinois
[6]Department of Cell and Molecular Biology, Northwestern University Feinberg School of Medicine, Chicago, Illinois

Abstract Cellular mechanisms causing cardiac hypertrophy are currently under intense investigation. We report a novel finding in the TGFβ inducible early gene (TIEG) null mouse implicating TIEG1 in cardiac hypertrophy. The $TIEG^{-/-}$ knock-out mouse was studied. Male mice age 4–16 months were characterized (N = 86 total) using echocardiography, transcript profiling by gene microarray, and immunohistochemistry localized upregulated genes for determination of cellular mechanism. The female mice (N = 40) did not develop hypertrophy or fibrosis. The $TIEG^{-/-}$ knock-out mouse developed features of cardiac hypertrophy including asymmetric septal hypertrophy, an increase in ventricular size at age 16 months, an increase (214%) in mouse heart/weight body weight ratio $TIEG^{-/-}$, and an increase in wall thickness in $TIEG^{-/-}$ mice of (1.85 ± 0.21 mm), compared to the control (1.13 ± 0.15 mm, $P < 0.04$). Masson Trichrome staining demonstrated evidence of myocyte disarray and myofibroblast fibrosis. Microarray analysis of the left ventricles demonstrated that $TIEG^{-/-}$ heart tissues expressed a 13.81-fold increase in pituitary tumor-transforming gene-1 (*Pttg1*). An increase in Pttg1 and histone H3 protein levels were confirmed in the $TIEG^{-/-}$ mice hearts tissues. We present evidence implicating TIEG and possibly its target gene, *Pttg1*, in the development of cardiac hypertrophy in the TIEG null mouse. J. Cell. Biochem. 100: 315–325, 2007.

Key words: TIEG; cardial hypertrophy; PTTG-1

Cardiomyopathies are complex disease processes which can have heterogeneous pathologic presentations. Numerous studies evaluating the cellular mechanisms and genetic factors have contributed profoundly to the overall understanding of this disease process. Transgenic models exist that overexpress mutant myosin heavy chains [Vikstrom et al., 1995; Marian et al., 1999], mutant cardiac troponin T [Oberst et al., 1998; Tardiff et al., 1998], mutant myosin binding protein-C [Yang et al., 1998] or cardiac troponin I [James et al., 2000], and the myosin (Arg403Gln) mutation produced by homologous recombination [Geisterfer-Lowrance et al., 1996]. Transgenic and knock-out mouse models involving signaling pathways for stress-induced hypertrophy include calcinuerin [Molkentin et al., 1998], modulatory

Nalini M. Rajamannan and Malayannan Subramaniam are the co-first authors.

Grant sponsor: US National Institutes of Health; Grant numbers: RO1 DE14036, 1K08HL073927-01; Grant sponsor: the Mayo Foundation.

*Correspondence to: Nalini M. Rajamannan, MD, Northwestern University Feinberg School of Medicine, 300 E Chicago Ave., Tarry 12-717, Chicago, IL 60611.
E-mail: n-rajamannan@northwestern.edu

Received 13 May 2006; Accepted 7 June 2006
DOI 10.1002/jcb.21049

calcineurin-interacting protein (MCIP) 1 [Vega et al., 2003], class II histone deacetylases (HDACs) [Zhang et al., 2002], homeobox only protein (HOP) [Kook et al., 2003], and MEF2 [Lin et al., 1997]. These important animal models demonstrate features of hypertrophic cardiomyopathy: ventricular hypertrophy, myocyte disarray, and fibrosis. However, the fundamental cellular mechanisms involved in this disease are not fully known and additional hypertrophic signaling cascades likely exist.

In 1995, our laboratory discovered the TGFβ inducible early gene-1 (*TIEG1*) which was characterized as a Krüppel-like zinc-finger transcription factor, expressed in normal human myocardium and in many, but not all, other tissues [Subramaniam et al., 1995, 1998]. The gene is also induced in human osteoblasts by estrogen and by members of the transforming growth factor-β (TGFβ) superfamily, including TGFβ and bone morphogenetic protein-2 (BMP-2) [Subramaniam et al., 1995] which utilize the Smad signaling pathway [Johnsen et al., 2002b]. Interestingly, the TGFβ1 signaling pathway has been implicated in cardiomyocyte growth and fibrosis which are characteristics of cardiac hypertrophy [Li et al., 1998]. The TIEG was discovered in one of our laboratories (MS and TCS) and identified as a transcript that is rapidly induced within 60 min of TGFβ, BMP, or EGF treatment in human osteoblasts, pancreatic, hepatic, and lung epithelial cells, as well as breast and pancreatic carcinomas [Blok et al., 1995; Subramaniam et al., 1995; Tachibana et al., 1997; Tau et al., 1998; Chalaux et al., 1999; Ribeiro et al., 1999; Hefferan et al., 2000a]. In this study, we report that the TIEG null mice develop a cardiac hypertrophic phenotype with asymmetric hypertrophy, interstitial fibrosis, and myocyte disarray.

MATERIALS AND METHODS

Generation and Analysis of TIEG1$^{-/-}$ Mice

To discern the functional role(s) of the *TIEG1*, we generated mice that lack the *TIEG1* gene (TIEG$^{-/-}$ animals). TIEG1 null embryonic stem cells were developed in collaboration with Incyte Genomics (St. Louis, MO) by targeted disruption of 2.3 kb of TIEG promoter and 5′-flanking sequences, exon-1,2, and a portion of exon-3. Mice homozygous for this disruption fail to express TIEG mRNA and protein [Subramaniam et al., 2005].

Experimental Animal Model

Experimental studies were performed evaluating the control mice TIEG$^{+/+}$ and TIEG$^{-/-}$ mice under the IACUC approval (A30504). The male mice were studied from age 4 to 16 months (N = 86) total. The mice were weighed before sacrifice an echocardiogram was performed as outlined below, and then euthanization by CO_2. All experiments were performed in an animal facility accredited by the Association for Assessment and Accreditation of Laboratory Animal Care, Inc. (ACUC-A15803). Immediately after dissection, the hearts were weighed. The ventricles were fixed in formalin and embedded in paraffin. Paraffin embedded sections (6 μm) were cut and stained with Masson Trichrome stain for histopathologic examination performed on the male and female mice. Longitudinal sections taken from the heart at the time of sacrifice were placed in Trump's fixative and analyzed for transmission electron microscopy as performed in previous studies [Rajamannan et al., 2002].

Echocardiography

Before sacrificing the TIEG$^{-/-}$ mice, transthoracic imaging was performed using M-mode ultrasound imaging from parasternal short axis views. All imaging was performed using a Vivid FiVe ultra-sound machine and a 15 MHz linear multi-frequency phased array probe (GE Vingmed, Horten, Norway). Fractional shortening was calculated from the M-Mode measurements (Echopac version 6.25b software, GE Vingmed). (N = 40 were studied including female TIEG$^{+/+}$ and TIEG$^{-/-}$ mice as controls to determine if hypertrophy develops in the female mice.)

Gene Microarray

Total RNA was isolated using Trizol Reagent (Invitrogen) and 4 μg of RNA was used in microarray analysis on the mouse MOE430A microarray (Affymetrix, Santa Clara, CA) containing oligonucleotide probes for approximately 23,000 mouse sequences. Analysis of the gene expression profiles was performed using the GeneSpring 6.1 software (Silicon Genetics, Redwood City, CA). Only those genes differentially expressed >twofold are represented in the data analysis (N = 5 with replicates of N = 3 for the null male mice and N = 2 for the control male mice).

Reverse Transcriptase Polymerase Chain Reaction

The left ventricles from the 16-month-old mice hearts were frozen immediately for RNA extraction. Total RNA was isolated using the Trizol kit (Invitrogen). Reverse transcriptase polymerase chain reaction (RT-PCR) analysis was performed for the expression of TIEG1, HOP [Subramaniam et al., 1995; Kook et al., 2003], MEF2 [Lin et al., 1997], HDACII [Zhang et al., 2002], ANF [Rockman et al., 1991], BNP [Harada et al., 1998], SMAD7 and SMAD2 [Johnsen et al., 2002a], and Pttg1 [Pei and Melmed, 1997]. GAPDH expression was tested as a control (N = 20 were studied).

Immunofluorescence of Mouse Cardiac Tissues

Immunostaining of the mouse ventricles was performed to identify pituitary tumor-transforming gene-1 (*Pttg1*) and histone H3. Deparafinized slides were fixed in ice cold acetone for 10 min. Sections were washed twice in TBS and avidin/biotin block for 15 min. Sections were incubated with Pttg primary antibody (Santa Cruz, CA) diluted 1:50 or histone H3 antibody (Cell Signaling, Beverly, MA) at 1:50 and no antibody for a negative control for 1 h. Sections were rinsed and incubated in anti-rabbit biotinylated secondary antibody diluted 1:500 for 30 min. After secondary incubation, FITC-avidin D were placed on the slide for 30 min. Slides were counter-stained with DAPI for 30 min. Slides were rinsed in TBS and mount slides with gevatol mounting medium. Slides were visualized using the following confocal microscopy technique (N = 20 male and female mice were studied).

Confocal Immunofluorescence Measurements

In order to eliminate the significant background autofluorescence from the heart tissue, we performed detailed emission spectral fingerprinting on the Zeiss LSM510 laser scanning confocal equipped with the META module (Northwestern University Cell Imaging Facility, Chicago, IL). Specifically, we obtained the specific emission fingerprints of unstained heart tissue by acquiring a stack of spectrally resolved confocal images to eliminate the background autofluorescence of the myocyte tissues.

The Pttg1 Promoter and TIEG1 Regulation of this Promoter

PTTG promoter or pGL3 basic luciferase construct (1 μg) along with empty expression vector or TIEG expression vector (1 μg) were transfected into AKR2B mouse embryo fibroblasts. As an internal control for transfection efficiency 0.5 μg of renilla luciferase was also transfected. Following 24 h of transfection, the cell lysates were prepared and analyzed for dual luciferase activity.

RESULTS

Cardiac Hypertrophy in the TIEG$^{-/-}$ Male Mice

All parameters of the TIEG$^{-/-}$ mice hearts were compared to the wild-type control mice. Our initial observation was asymmetric left ventricular hypertrophy in the 16-month-old male TIEG$^{-/-}$ mice as demonstrated in the photograph of the longitudinal cross-section through each ventricle (Fig. 1, Panel A). We confirmed the finding of a (214%) increase in cardiac mass by the heart weight/body weight ratio TIEG$^{-/-}$ (9.44 ± 0.12 mg/g) versus control (4.40 ± 0.17 mg/g) as shown in the graph, Figure 1, Panel B. Figure 1 Panel C, demonstrates the low magnification histologic analysis of the experimental TIEG$^{-/-}$ mice compared to wild-type at age 16 months. The Masson Trichrome stain demonstrates large areas of fibrosis present in the TIEG$^{-/-}$ left ventricle compared to the wild-type control. We measured the anterior wall septal thickness by M-mode and found an increase in the TIEG$^{-/-}$ 16-month-old mice. The anterior wall measured 1.85 ± 0.21 mm compared to wild-type 1.13 ± 0.15 as shown in Figure 1, Panel D and Table I. Table I demonstrates the left ventricular echocardiographic data from the male and female mice. The female mice did not develop hypertrophy by echocardiography.

Masson Trichrome and Electron Microscopy of the TIEG Mice

Figure 2, Panels A1 and A2, is the Masson Trichrome stain of the 4-month-old male TIEG$^{-/-}$ mice compared to wild-type. There was no evidence of fibrosis in these mice at 4 months of age. Figure 2, Panels B1 and B2, demonstrates the marked interstitial fibrosis present in the left ventricles of the 16-month-old male TIEG$^{-/-}$ mice compared to the wild-type

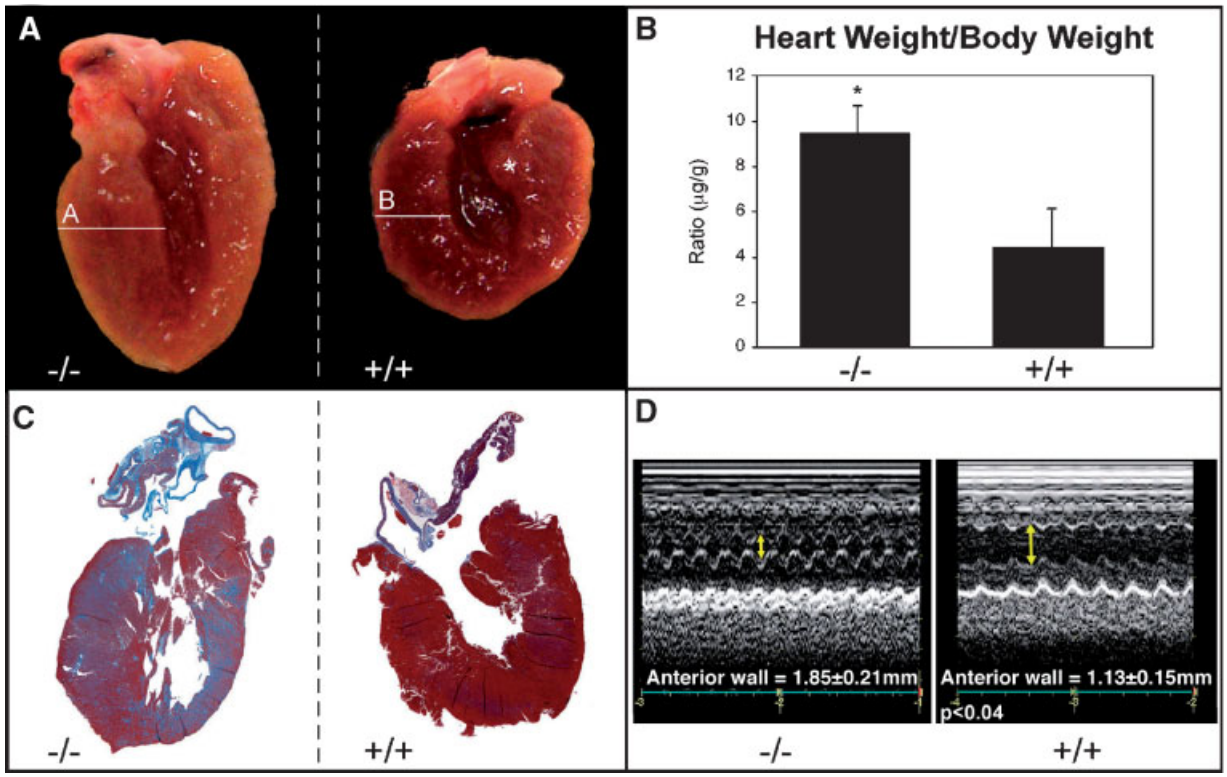

Fig. 1. Whole heart and M-mode echo. **Panel A**: TIEG$^{+/+}$ versus TIEG$^{-/-}$ photograph of the whole heart. **Panel B**: Heart weight/body weight ratio (mg/g). **Panel C**: TIEG$^{+/+}$ versus TIEG$^{-/-}$ Masson Trichrome stain of the longitudinal cross-section of the heart, (Mag 5×). **Panel D**: TIEG$^{+/+}$ versus TIEG$^{-/-}$ M-mode echocardiography, arrow points to the left ventricular cavity. The measurement below the M-mode demonstrates the anterior wall thickness.

control male mice. Figure 2, Panels C1 and C2, demonstrates by transmission electron microscopy that the TIEG$^{-/-}$ mice had a significantly abnormal sarcomeric architecture and myofibrillar disarray. The arrow points to the sarcomere Z lines in the control hearts and in the TIEG$^{-/-}$ heart. The female TIEG mice demonstrated no evidence of fibrosis in the hearts at any age as shown in female TIEG$^{-/-}$ mice as shown in Figure 2, Panels D1 and D2.

Gene Array and RT-PCR

Figure 3, Panel A demonstrates the RT-PCR for the known stress-induced hypertrophy genes and *SMAD7* and *SMAD2* genes. There were no differences in the gene expression for *HOP*, *MEF*, *HDAC*, *ANF*, *BNP*, *and SMAD7 and 2* in the TIEG$^{-/-}$ male mice compared to wild-type (TIEG$^{+/+}$) male mice. *TIEG1* was absent in the knock-out mice at 16 months. The gene microarray analysis is shown in Figure 3 Panel B, which identifies the genes with greater than threefold enhanced mRNA levels. Table II lists all of the genes that are up or downregulated in the gene microarray with increased mRNA levels. *Pttg1* displayed the greatest increase of 13.8-fold in the TIEG$^{-/-}$ mice compared to the TIEG$^{+/+}$ mice. We

TABLE I. Hemodynamic and Echocardiography Data From the TIEG$^{-/-}$ Versus TIEG$^{+/+}$ Mice

Echo data	Posterior wall/ diastole	Anterior wall/ diastole	End diastolic cavity	End systolic cavity	Fractional shortening
Male					
TIEG$^{-/-}$ mouse	1.38 ± 0.39	1.85 ± 0.12**	3.13 ± 1.55	1.8 ± 0.67	36.25 ± 17.54
TIEG$^{+/+}$ mouse	1.4 ± 0.17	1.13 ± 0.15	4.53 ± 0.06	2.76 ± 0.12	37.97 ± 1.76
Female					
TIEG$^{-/-}$ mouse	1.08 ± 0.15	0.82 ± 0.12	3.38 ± 0.95	2.37 ± 0.38	32.32 ± 9.49
TIEG$^{+/+}$ mouse	0.82 ± 0.15	0.76 ± 0.32	3.48 ± 0.95	2.05 ± 0.41	38.51 ± 5.23

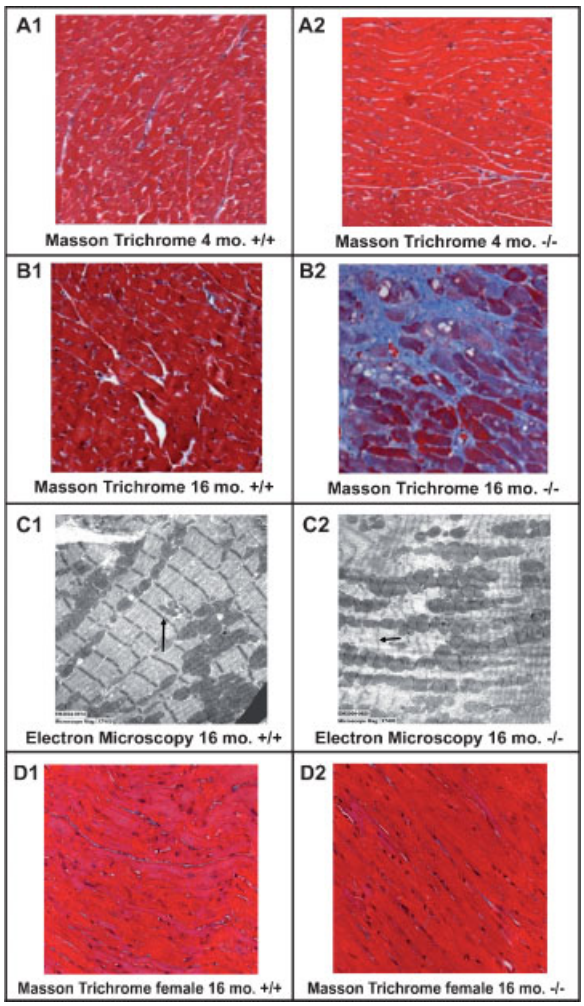

Fig. 2. Histologic analysis of the TIEG heart. **Panels A1** and **A2**: $TIEG^{+/+}$ versus $TIEG^{-/-}$ Masson Trichrome stain 4-month-old mice (low magnification 25×). **Panels B1** and **B2**: $TIEG^{+/+}$ versus $TIEG^{-/-}$ Masson Trichrome stain 4-month-old mice (low magnification 25×). **Panels C1** and **C2**: $TIEG^{+/+}$ versus $TIEG^{-/-}$ transmission electron microscopy, arrow points to the sarcomere Z lines (magnification 7,400×). **Panels D1** and **D2**: $TIEG^{+/+}$ versus $TIEG^{-/-}$ Masson Trichrome stain 16-month-old female mice (low magnification 25×).

confirmed the gene expression of *Pttg1* in the myocardium by RT-PCR in the 4 months and the 16 months male TIEG mice as shown in Figure 3, Panel C. Figure 3, Panel D, also shows an increase in Pttg1 protein expression also shown by the immunofluorescence in the 16-month-old $TIEG^{-/-}$ male mice as to the control. We also tested the negative control and found no Pttg1 expression. We quantified the Pttg-positive cardiac myocytes in the $TIEG^{-/-}$ hearts and found a marked increase in the positive staining myocyte cells (8.5 ± 2.08, $P < 0.001$) versus $TIEG^{+/+}$ hearts (0.00). There was no evidence of Pttg protein staining in the female $TIEG^{-/-}$ versus $TIEG^{+/+}$ mice at 4 months and 16 months (data not shown).

Effect of TIEG on Pttg1 Promoter Activity

The results obtained from gene array comparing the gene expression profiles of $TIEG^{+/+}$ and $TIEG^{-/-}$ heart tissues revealed that Pttg was highly expressed in $TIEG^{-/-}$ hearts, suggesting that TIEG negatively regulates Pttg gene expression. These results were further confirmed through RT-PCR analysis. To further determine if the regulation of Pttg gene expression by TIEG protein occur at the promoter level, we cloned the Pttg1 promoter, containing the 5′-flanking region (−1,321 to −3), in front of the luciferase reporter (See Fig. 3, Panel E) and performed transfection analyses. As shown in Figure 3, Panel F, when the Pttg promoter construct was transfected into AKR2B mouse embryo fibroblasts, an increased promoter activity was observed compared to the basic luciferase construct. Interestingly, when the promoter construct was co-transfected with TIEG expression vector, a 60–70% drop in the promoter activity was observed. These results clearly suggest that TIEG protein negatively regulates Pttg gene expression by binding to the regulatory sequences of Pttg promoter. This provides a potential mechanistic reason for the large increase in Pttg1 expression in the $TIEG^{-/-}$ hearts compared to the $TIEG^{+/+}$ hearts.

Evidence for Histone H3 Expression in the Cardiomyocytes

Figure 4, Panel A, demonstrates, by Western blot analysis, that the expression of histone H3 in the $TIEG^{-/-}$ hearts was markedly increased as compared to the $TIEG^{+/+}$ hearts. Figure 4, Panel B is the spectral profiles of background autofluorescence from unstained heart tissue. Tissue was excited with 405 nm and 488 nm lasers, and images were taken using Zeiss META module from 427 nm to 530 nm, with 10.7 nm wavelength intervals (spectral resolution). Any pixel with spectra matching the nonspecific autofluorescence background were spectrally removed from the final image, thus obviating the need to perform background subtraction that could skew the resultant fluorescent intensities. The multiple reference spectra were stored in the spectral database for

TABLE II. Gene Microarray Data From the TIEG$^{-/-}$ Versus TIEG$^{+/+}$ Left Ventricular Hearts

Gene name	Description	Accession	Fold change
Pttg1	Pituitary tumor-transforming 1	AF069051	13.81
Myl7	Myosin, light polypeptide 7, regulatory	NM_022879	5.66
Pttg1	AV105428 Mus musculus liver C57BL/6J	AV105428	4.93
Myl4	Myosin, light polypeptide 4, alkali; atrial, embryonic	NM_010858	3.77
1500035H01Rik	RIKEN cDNA 1500035H01 gene	NM_023831	3.56
Wif1	Wnt inhibitory factor 1	BC004048	3.41
Anxa8	Annexin A8	NM_013473	3.03
Hamp	Hepcidin anti-microbial peptide	NM_032541	2.79
E2f5	E2F transcription factor 5	BC003220	2.50
Ppt1	Palmitoyl-protein thioesterase 1	AF326558	2.43
Dbp	BB550183 RIKEN full-length enriched	BB550183	2.42
2210407C18Rik	RIKEN cDNA 2210407C18 gene	BC019553	2.42
Ppat	Phosphoribosyl pyrophosphate amidotransferase	BG064988	2.28
Cyfip2	Cytoplasmic FMR1 interacting protein 2	NM_133769	2.21
Nr2f2	Nuclear receptor subfamily 2, F2	NM_009697	2.20
Dkk3	Dickkopf homolog 3 (Xenopus laevis)	AK004853	2.17
Myl1	Myosin, light polypeptide 1, alkali; atrial, embryonic	AK003182	2.14
Ptpn2	Protein tyrosine phosphatase, non-receptor type 2	AV167543	2.13
1110008H02Rik	Mus musculus 18-day embryo body	AW988981	2.13
Acadl	Acetyl-coenzyme A dehydrogenase, long-chain	BB728073	2.01
Nov	Nephroblastoma overexpressed gene	X96585	2.01
Matn1	Matrilin 1, cartilage matrix protein 1	NM_010769	0.49
	H3044G12-3 NIA Mouse 15K cDNA	BG066678	0.49
Ddx3y	DEAD box polypeptide 3, Y-linked	AA210261	0.48
Il15	Interleukin 15	NM_008357	0.48
Pfkfb2	6-phosphofructo-2-kinase/fructose-2,6-biphosphatase 2	NM_008825	0.47
Tnfrsf12a	Tumor necrosis factor receptor superfamily, member 12a	NM_013749	0.46
Trfr	Transferrin receptor	NM_011638	0.45
Mic2l1	BB334959 RIKEN full-length enriched	BB334959	0.45
Pam	Peptidylglycine alpha-amidating monooxygenase	NM_013626	0.43
Ndr4	N-myc downstream regulated 4	AV006122	0.43
Sema4a	X85991 semaphorin B	BB114323	0.43
Nras	Neuroblastoma ras oncogene	NM_010937	0.43
Prdx2	Peroxiredoxin 2	AK011963	0.42
AI255170	Expressed sequence AI255170	BE134496	0.42
Ndr4	N-myc downstream regulated 4	Al837704	0.38
Tnfrsf12a	Tumor necrosis factor receptor superfamily, member 12a	NM_013749	0.38
Amacr	Alpha-methylacyl-CoA racemase	NM_008537	0.38
	Mus musculus cDNA', mRNA sequence.	BF580235	0.31
Terf1	Telomeric repeat binding factor 1	BG142548	0.30
Ddx3y	DEAD (Asp-Glu-Ala-Asp) box polypeptide 3, Y-linked	BB667072	0.27
Sdc2	Syndecan 2	NM_008304	0.26
Eif2s3y	Eukaryotic translation initiation factor 2, subunit 3, Y-linked	NM_012011	0.26
Ddx3y	DEAD box polypeptide 3, Y-linked	AJ007376	0.24
	602099052F1 NCI_CGAP_Co24	BF580235	0.23
TIEG1	TGFB inducible early growth response 1	NM_013692	0.11

subsequent analyses. Similar procedures were performed on samples singly stained with either DAPI (for nuclei) or fluorescein-conjugated anti-histone 3 antibody. Figure 4, Panel C, demonstrates the immunofluorescence for histone H3 localizing to cardiac myocytes only in the TIEG null mice cardiomyocytes. These allowed us to obtain the unique spectral fingerprints of DAPI and FITC in the heart tissue as shown in Figure 4, Panel C. We then directly characterized the extent and pattern of histone H3 nuclear localization by performing double color immunofluorescence using DAPI and the fluorescein-conjugated anti-histone antibody as shown in the overlay image in Figure 4, Panel C. We quantified the histone-positive cardiac myocytes in the male TIEG$^{-/-}$ hearts (14.33 ± 4.93, $P < 0.001$) versus TIEG$^{+/+}$ hearts (0.00) and found a statistical increase in the male TIEG$^{-/-}$ hearts. There was no evidence of histone H3 staining in the female mice (data not shown).

Potential Mechanism of TIEG in Cardiac Myocytes

Figure 5, displays a model showing a potential pathway of how TIEG might regulate development of hypertrophic cardiomyopathy in the hearts of the TIEG null mice. The TIEG knock-out mouse fully demonstrates the phenotypic characteristics of hypertrophic cardiomyopathy with the development of late onset, severe, asymmetric cardiac hypertrophy in the absence of hypertension. This process is accompanied by myofibrillar disarray, and fibrosis. This supports the model that TIEG acts as a repressor of Pttg1 gene expression which, in turn, results in the cardiac suppression of

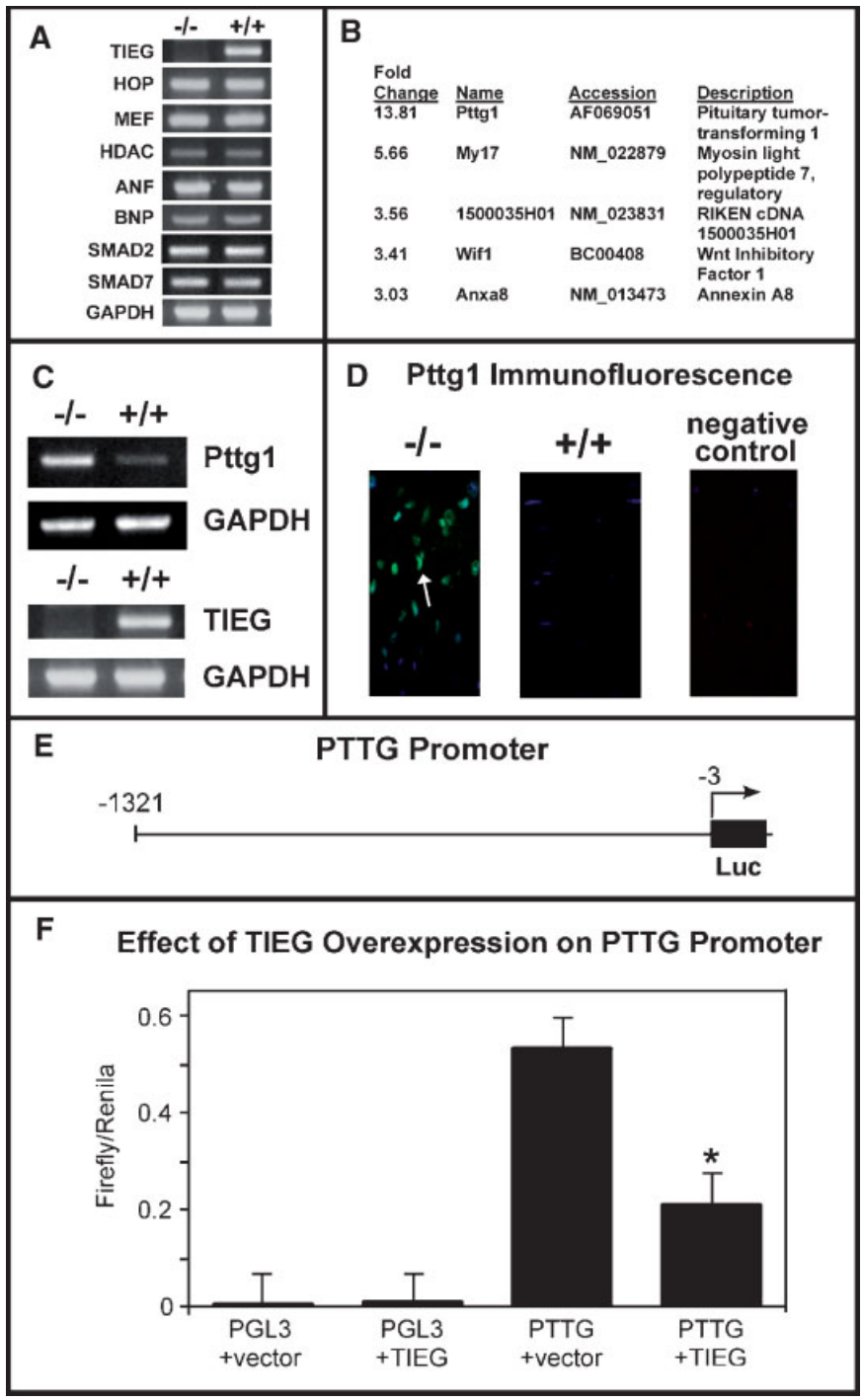

Fig. 3. Gene microarray and RT-PCR. **Panel A**: $TIEG^{+/+}$ versus $TIEG^{-/-}$ RT-PCR of the known stress-induced hypertrophy genes and *SMAD* genes. **Panel B**: $TIEG^{+/+}$ versus $TIEG^{-/-}$ Gene Array from the left ventricle of genes upregulated >threefold. **Panel C**: $TIEG^{+/+}$ versus $TIEG^{-/-}$ RT-PCR for Pttg1 and TIEG in the 4-month and 16-month-old male mice. **Panel D**: Immunohistochemistry for *Pttg1* in the cardiomyocytes and the negative control. **Panel E**: Model of the Pttg1 promoter. **Panel F**: PTTG promoter or pGL3 basic luciferase construct (1 μg) along with empty expression vector and/or TIEG expression vector (1 μg) were transfected into AKR2B mouse embryo fibroblasts demonstrating the reduction in PTTG promoter activity with the co-expression of the TIEG vector.

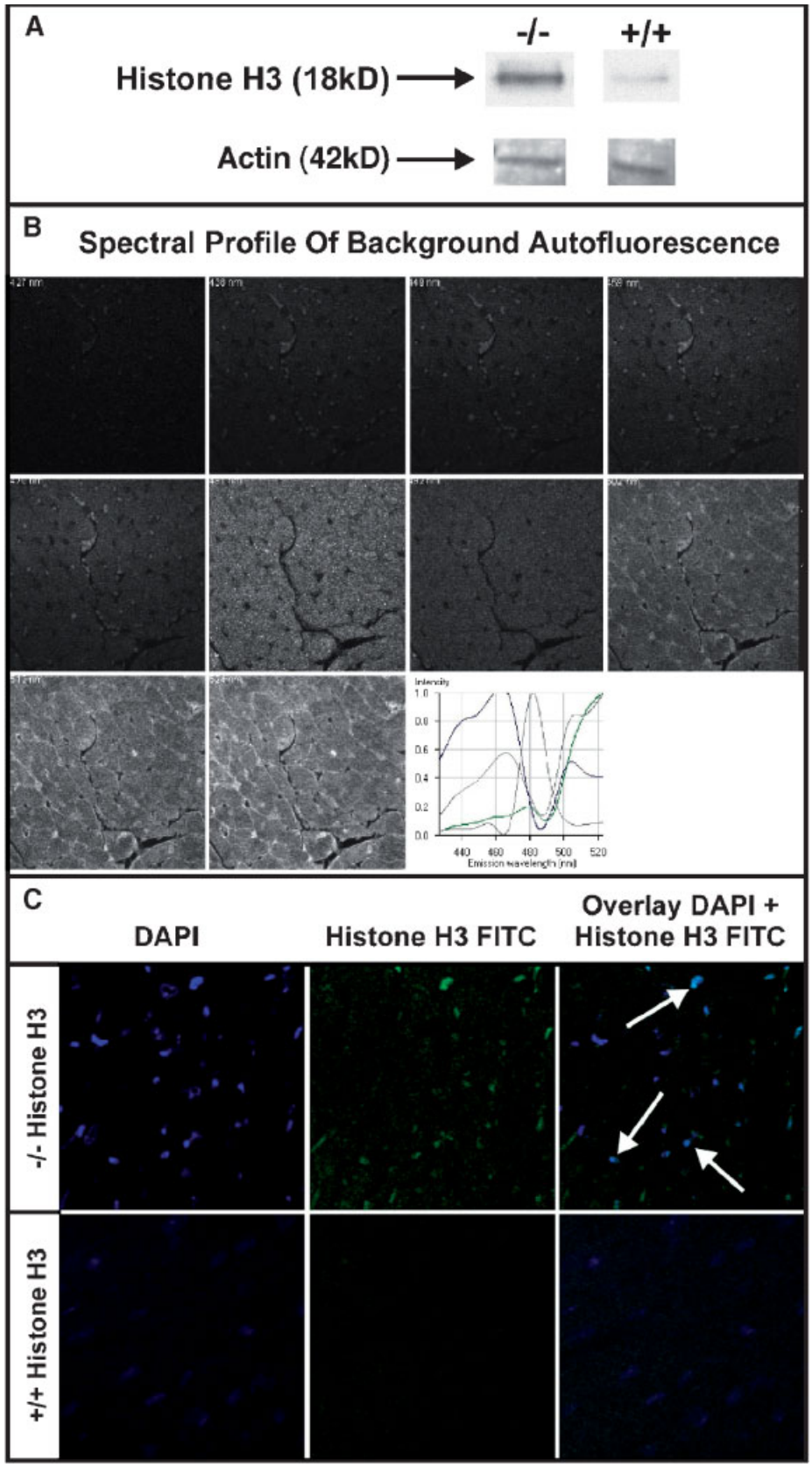

Fig. 4. Immunofluorescence of histone H3 and Western blot analysis. **Panel A**: Western blot analysis for histone H2. **Panel B**: Spectral profile of background autofluorescence. **Panel C**: Immunofluorescence of histone H3.

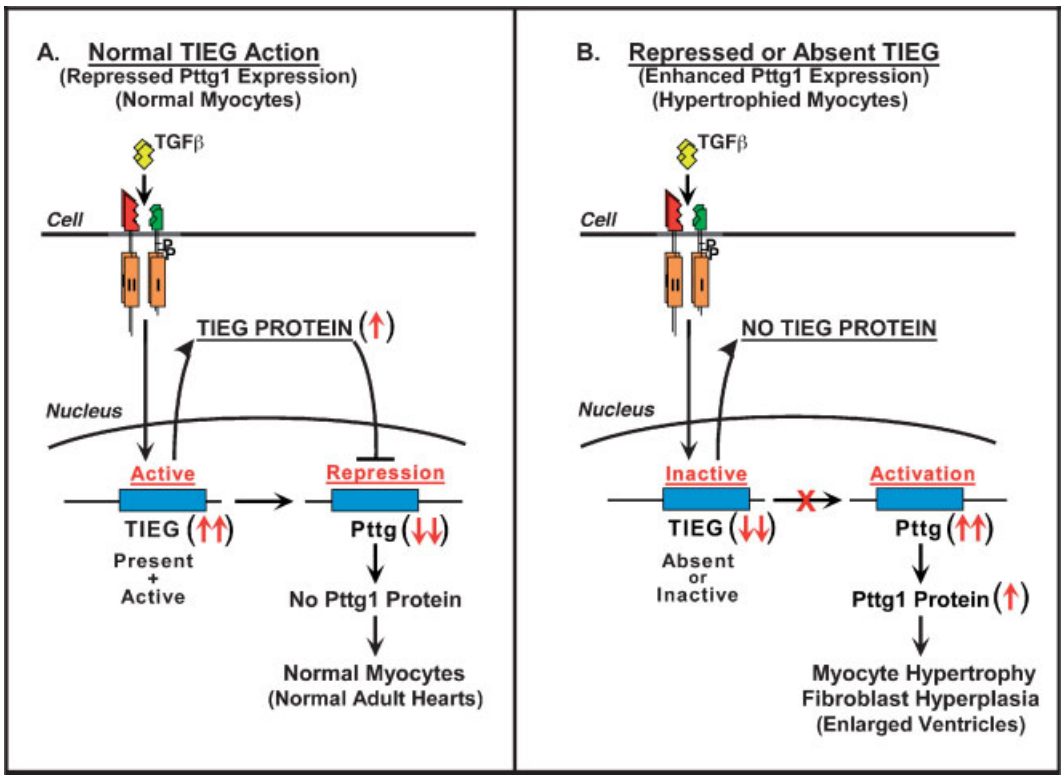

Fig. 5. Potential mechanism of TIEG and cardiac hypertrophy. **Panel A**: Normal TIEG action. **Panel B**: Repressed or absent TIEG.

cardiac myocyte hypertrophy Figure 5, Panel A. In the absence of TIEG, Pttg is upregulated and myocyte hypertrophy progresses and fibrosis develops as shown in Figure 5, Panel B.

DISCUSSION

The TIEG knock-out mouse demonstrates the development of late onset, severe, cardiac hypertrophy in the absence of hypertension accompanied by myofibrillar disarray, and fibrosis.

TIEG is a member of the 16-member Krüppel-like factor (KLF) family of three zinc-finger proteins [Philipsen and Suske, 1999; Turner and Crossley, 1999; Dang et al., 2000]. These factors bind to the GC rich elements in gene promoters to regulate more than 1,000 genes involved in cell growth differentiation and apoptosis [Liu et al., 1996; Cook et al., 1999; Zhang et al., 2001]. The *TIEG* gene encodes a 480 amino acid (72 kDa) protein with a unique amino-terminal end which distinguishes it from an early growth response-α (*EGRα*) gene produced from an alternative promoter [Blok et al., 1995; Subramaniam et al., 1995; Fautsch et al., 1998a,b]. The overexpression of TIEG has been shown to mimic the effects of TGFβ in human cancer cells [Tachibana et al., 1997; Hefferan et al., 2000b]. The ability of TIEG to enhance TGFβ actions and Smad pathway is Smad-dependent since TIEG has no effect on Smad binding element transcription in the absence of Smad4 expression or when an inhibitory Smad protein, Smad7, is overexpressed [Johnsen et al., 2002a,b]. In this model we tested for the following reported gene markers for cardiac hypertrophy and whether these markers represent potential pathways regulated by *TIEG*: *HOP*, *MEF*, *HDAC*, *ANF*, *BNP*, *and SMAD7 and 2*. Interestingly, we found no differences in the expression of these genes in the TIEG$^{-/-}$ male mice compared to wild-type male mice. We then examined for changes in gene expression in the left ventricles by gene array and found a significant increase in the expression of *Pttg1* also known as securin. *Pttg1* was originally cloned from rat pituitary gland [Pei and Melmed, 1997]. Pttg1 is known to be regulated by FGF secretion and regulates sister chromatid separation during mitosis [Zhou and Olson, 1994]. Pttg1 has also been implicated in

inducing hypertrophy in cells [Heaney et al., 1999]. In addition, the *Pttg1* gene promoter contains several Sp1 binding sites [Pei, 1998]. Previously, we demonstrated that TIEG1 can in fact bind to Sp1 sequences in the *Smad7* promoter and downregulate *Smad7* transcription [Johnsen et al., 2002a]. In this study, we demonstrate that overexpression of TIEG with the Pttg promoter reduces the promoter activity, implicating a similar mechanism that TIEG binds to the Sp1 binding site in the Pttg promoter. We propose a final common pathway model whereby TIEG1 acts as a hypertrophy suppressor signaling molecule normally binds to and downregulates *Pttg1* via binding to Sp1 sites. This model is a novel model to demonstrate interstitial fibrosis in the male mouse and not the female TIEG null mouse. This model of fibrosis in the male null mouse represents the potential for a universal mechanism in these cells with the lack of TIEG. Normal function of TIEG has been identified as a transcript that is rapidly induced in a number of normal cells, normal tissues, and carcinomas. In the absence of TIEG, *Pttg1* is dramatically upregulated and the hypertrophic process ensues and fibrosis develops in the hearts. There may be a dual pathway to inhibit fibrosis when TIEG is present. The first is the normal function of TIEG in these cells and second is the effect of estrogen inhibiting fibrosis. This study describes a novel, genetic-based model including an important signaling pathway involving the development of cardiac hypertrophy and interstitial fibrosis. Studies with this model should elucidate novel molecular pathways involved in the development of cardiac hypertrophy.

ACKNOWLEDGMENTS

This work was supported by the US National Institutes of Health (RO1 DE14036), and a grant from the US National Institutes of Health (1K08HL073927-01), the Mayo Foundation and Northwestern University. The authors thank Kay Rasmussen, Genevieve Gorny, Margaret Springett, and Frank Caira for their outstanding technical support.

REFERENCES

Blok LJ, Grossmann ME, Perry JE, Tindall DJ. 1995. Characterization of an early growth response gene, which encodes a zinc finger transcription factor, potentially involved in cell cycle regulation. Mol Endocrinol 9(11):1610–1620.

Chalaux E, Lopez-Rovira T, Rosa JL, et al. 1999. A zinc-finger transcription factor induced by TGF-beta promotes apoptotic cell death in epithelial Mv1Lu cells. FEBS Lett 457(3):478–482.

Cook T, Gebelein B, Belal M, Mesa K, Urrutia R. 1999. Three conserved transcriptional repressor domains are a defining feature of the TIEG subfamily of Sp1-like zinc finger proteins. J Biol Chem 274(41):29500–29504.

Dang DT, Pevsner J, Yang VW. 2000. The biology of the mammalian Kruppel-like family of transcription factors. Int J Biochem Cell Biol 32(11–12):1103–1121.

Fautsch MP, Vrabel A, Rickard D, Subramaniam M, Spelsberg TC, Wieben ED. 1998a. Characterization of the mouse TGFbeta-inducible early gene (TIEG): Conservation of exon and transcriptional regulatory sequences with evidence of additional transcripts. Mamm Genome 9(10):838–842.

Fautsch MP, Vrabel A, Subramaniam M, Hefferen TE, Spelsberg TC, Wieben ED. 1998b. TGFbeta-inducible early gene (TIEG) also codes for early growth response alpha (EGRalpha): Evidence of multiple transcripts from alternate promoters. Genomics 51(3):408–416.

Geisterfer-Lowrance AA, Christe M, Conner DA, et al. 1996. A mouse model of familial hypertrophic cardiomyopathy. Science 272(5262):731–734.

Harada M, Saito Y, Kuwahara K, et al. 1998. Interaction of myocytes and nonmyocytes is necessary for mechanical stretch to induce ANP/BNP production in cardiocyte culture. J Cardiovasc Pharmacol 31(Suppl 1):S357–S359.

Heaney AP, Horwitz GA, Wang Z, Singson R, Melmed S. 1999. Early involvement of estrogen-induced pituitary tumor transforming gene and fibroblast growth factor expression in prolactinoma pathogenesis. Nat Med 5(11): 1317–1321.

Hefferan TE, Subramaniam M, Khosla S, Riggs BL, Spelsberg TC. 2000a. Cytokine-specific induction of the TGF-beta inducible early gene (TIEG): Regulation by specific members of the TGF-beta family. J Cell Biochem 78(3):380–390.

Hefferan TE, Reinholz GG, Rickard DJ, et al. 2000b. Overexpression of a nuclear protein, TIEG, mimics transforming growth factor-beta action in human osteoblast cells. J Biol Chem 275(27):20255–20259.

James J, Zhang Y, Osinska H, et al. 2000. Transgenic modeling of a cardiac troponin I mutation linked to familial hypertrophic cardiomyopathy. Circ Res 87(9): 805–811.

Johnsen SA, Subramaniam M, Janknecht R, Spelsberg TC. 2002a. TGFbeta inducible early gene enhances TGFbeta/Smad-dependent transcriptional responses. Oncogene 21(37):5783–5790.

Johnsen SA, Subramaniam M, Katagiri T, Janknecht R, Spelsberg TC. 2002b. Transcriptional regulation of Smad2 is required for enhancement of TGFbeta/Smad signaling by TGFbeta inducible early gene. J Cell Biochem 87(2):233–241.

Kook H, Lepore JJ, Gitler AD, et al. 2003. Cardiac hypertrophy and histone deacetylase-dependent transcriptional repression mediated by the atypical homeodomain protein Hop. J Clin Invest 112(6):863–871.

Li G, Li RK, Mickle DA, et al. 1998. Elevated insulin-like growth factor-I and transforming growth factor-beta 1

and their receptors in patients with idiopathic hypertrophic obstructive cardiomyopathy. A possible mechanism. Circulation 98(Suppl 19):II144–II149; discussion II9-I50.

Lin Q, Schwarz J, Bucana C, Olson EN. 1997. Control of mouse cardiac morphogenesis and myogenesis by transcription factor MEF2C. Science 276(5317):1404–1407.

Liu C, Calogero A, Ragona G, Adamson E, Mercola D. 1996. EGR-1, the reluctant suppression factor: EGR-1 is known to function in the regulation of growth, differentiation, and also has significant tumor suppressor activity and a mechanism involving the induction of TGF-beta1 is postulated to account for this suppressor activity. Crit Rev Oncog 7(1–2):101–125.

Marian AJ, Wu Y, Lim DS, et al. 1999. A transgenic rabbit model for human hypertrophic cardiomyopathy. J Clin Invest 104(12):1683–1692.

Molkentin JD, Lu JR, Antos CL, et al. 1998. A calcineurin-dependent transcriptional pathway for cardiac hypertrophy. Cell 93(2):215–228.

Oberst L, Zhao G, Park JT, et al. 1998. Dominant-negative effect of a mutant cardiac troponin T on cardiac structure and function in transgenic mice. J Clin Invest 102(8): 1498–1505.

Pei L. 1998. Genomic organization and identification of an enhancer element containing binding sites for multiple proteins in rat pituitary tumor-transforming gene. J Biol Chem 273(9):5219–5225.

Pei L, Melmed S. 1997. Isolation and characterization of a pituitary tumor-transforming gene (PTTG). Mol Endocrinol 11(4):433–441.

Philipsen S, Suske G. 1999. A tale of three fingers: The family of mammalian Sp/XKLF transcription factors. Nucleic Acids Res 27(15):2991–3000.

Rajamannan NM, Springett MJ, Pederson LG, Carmichael SW. 2002. Localization of caveolin 1 in aortic valve endothelial cells using antigen retrieval. J Histochem Cytochem 50(5):617–628.

Ribeiro A, Bronk SF, Roberts PJ, Urrutia R, Gores GJ. 1999. The transforming growth factor beta(1)-inducible transcription factor TIEG1, mediates apoptosis through oxidative stress. Hepatology 30(6):1490–1497.

Rockman HA, Ross RS, Harris AN, et al. 1991. Segregation of atrial-specific and inducible expression of an atrial natriuretic factor transgene in an in vivo murine model of cardiac hypertrophy.[erratum appears in Proc Natl Acad Sci USA 1991 Nov 1;88(21):9907]. Proc Natl Acad Sci USA 88(18):8277–8281.

Subramaniam M, Harris SA, Oursler MJ, Rasmussen K, Riggs BL, Spelsberg TC. 1995. Identification of a novel TGF-beta-regulated gene encoding a putative zinc finger protein in human osteoblasts. Nucleic Acids Res 23(23):4907–4912.

Subramaniam M, Hefferan TE, Tau K, et al. 1998. Tissue, cell type, and breast cancer stage-specific expression of a TGF-beta inducible early transcription factor gene. J Cell Biochem 68(2):226–236.

Subramaniam MG, Gorny G, Johnsen SA, Monroe DG, Evans GL, Fraser DG, Rickard DJ, Rasmussen K, van Deursen J, Turner RT, Oursler MJ, Spelsberg TC. 2005. TIEG1 null mouse-derived osteoblasts are defective in mineralization and in support of osteoclast differentiation in vitro. Molec Cell Biol 25:1191–1199.

Tachibana I, Imoto M, Adjei PN, et al. 1997. Overexpression of the TGFbeta-regulated zinc finger encoding gene, TIEG, induces apoptosis in pancreatic epithelial cells. J Clin Invest 99(10):2365–2374.

Tardiff JC, Factor SM, Tompkins BD, et al. 1998. A truncated cardiac troponin T molecule in transgenic mice suggests multiple cellular mechanisms for familial hypertrophic cardiomyopathy. J Clin Invest 101(12): 2800–2811.

Tau KR, Hefferan TE, Waters KM, et al. 1998. Estrogen regulation of a transforming growth factor-beta inducible early gene that inhibits deoxyribonucleic acid synthesis in human osteoblasts. Endocrinology 139(3):1346–1353.

Turner J, Crossley M. 1999. Mammalian Kruppel-like transcription factors: More than just a pretty finger. Trends Biochem Sci 24(6):236–240.

Vega RB, Bassel-Duby R, Olson EN. 2003. Control of cardiac growth and function by calcineurin signaling. J Biol Chem 278(39):36981–3694.

Vikstrom KL, Factor SM, Leinwand LA. 1995. A murine model for hypertrophic cardiomyopathy. Z Kardiol 84(Suppl 4):49–54.

Yang Q, Sanbe A, Osinska H, Hewett TE, Klevitsky R, Robbins J. 1998. A mouse model of myosin binding protein C human familial hypertrophic cardiomyopathy. J Clin Invest 102(7):1292–1300.

Zhang JS, Moncrieffe MC, Kaczynski J, Ellenrieder V, Prendergast FG, Urrutia R. 2001. A conserved alpha-helical motif mediates the interaction of Sp1-like transcriptional repressors with the corepressor mSin3A. Mol Cell Biol 21(15):5041–5049.

Zhang CL, McKinsey TA, Olson EN. 2002. Association of class II histone deacetylases with heterochromatin protein 1: potential role for histone methylation in control of muscle differentiation. Mol Cell Biol 22(20):7302–7312.

Zhou J, Olson EN. 1994. Dimerization through the helix-loop-helix motif enhances phosphorylation of the transcription activation domains of myogenin. Mol Cell Biol 14(9):6232–6243.